Air-Cooled Heat Exchanger for High-Temperature Power Electronics

Preprint

S. K. Waye, J. Lustbader, M. Musselman, and C. King
National Renewable Energy Laboratory

NOTICE

This report is available at no cost from the National Renewable Energy Laboratory (NREL) at www.nrel.gov/publications.

Available electronically at SciTech Connect http:/www.osti.gov/scitech

Available for a processing fee to U.S. Department of Energy and its contractors, in paper, from:

> U.S. Department of Energy
> Office of Scientific and Technical Information
> P.O. Box 62
> Oak Ridge, TN 37831-0062
> OSTI http://www.osti.gov
> Phone: 865.576.8401
> Fax: 865.576.5728
> Email: reports@osti.gov

Available for sale to the public, in paper, from:

> U.S. Department of Commerce
> National Technical Information Service
> 5301 Shawnee Road
> Alexandra, VA 22312
> NTIS http://www.ntis.gov
> Phone: 800.553.6847 or 703.605.6000
> Fax: 703.605.6900
> Email: orders@ntis.gov

Air-Cooled Heat Exchanger for High-Temperature Power Electronics

Scot K. Waye, Jason Lustbader, Matthew Musselman, and Charles King

National Renewable Energy Laboratory
Golden, CO, 80401, USA, 303-275-4454, scot.waye@nrel.gov

Abstract — **This work demonstrates a direct air-cooled heat exchanger strategy for high-temperature power electronic devices with an application specific to automotive traction drive inverters. We present experimental heat dissipation and system pressure curves versus flow rate for baseline and optimized sub-module assemblies containing two ceramic resistance heaters that provide device heat fluxes. The maximum allowable junction temperature was set to 175°C. Results were extrapolated to the inverter scale and combined with balance-of-inverter components to estimate inverter power density and specific power. The results exceeded the goal of 12 kW/L and 12 kW/kg for power density and specific power, respectively.**

Index Terms — **Electronic packaging thermal management, electronics cooling, thermal management of electronics, wide band gap semiconductors**

I. INTRODUCTION

The low specific heat, density, and conductivity of air make it a relatively poor heat transfer fluid; however, it is benign, does not have to be carried, and does not have to be replaced. Air is also a dielectric, so it can come into direct contact with the chip, although that approach is not proposed in this research. For automotive applications, an air-cooled inverter provides a pathway for eliminating intermediate liquid cooling loops and a liquid–air heat exchanger. All heat from the vehicle is eventually rejected to ambient air.

To use air as a coolant for power electronics, a larger temperature difference is beneficial to increase the heat flux. Current silicon devices have maximum allowable junction temperatures between 125°C and 150°C [1]-[2] and may reach 175°C in the future. Wide-bandgap devices, such as silicon carbide and gallium nitride semiconductors, can operate at junction temperatures that exceed 200°C to increase device efficiency [3]-[5], although higher temperatures also raise concerns of device and packaging reliability. Air cooling for electronics is used for many applications, such as mainframes, supercomputers [6], and many other electronic products [7]. For automotive applications, several companies have produced air-cooled inverters or prototypes, but these are either for low-power (12.4 kW) applications [8], have low production volumes and relatively low power densities [9], or are not yet commercially available [10]. Inverters using silicon carbide operating at high ambient temperatures (under-hood temperatures of 120°C) are being developed [11]-[12].

II. APPROACH

A baseline air-cooled heat exchanger consisting of an aluminum heat sink with equally spaced rectangular channels was proposed [13]. Devices would be mounted to both sides to use the channel wall fins more effectively. The design incorporated nine modules for a full inverter with a 30-kW continuous and 55-kW peak power (for 18 seconds) output. This design did not meet targeted 12-kW/L power density and 12-kW/kg specific power requirements, proposed as 2015 targets by U.S. DRIVE electrical and electronics technical team [14]. For this size inverter and number of devices, the total heat loss was conservatively estimated to be 2.7 kW (using device loss information and analytical equations) [15].

Through a parametric computational fluid dynamics study, the heat sink was optimized for weight and volume by varying geometric parameters, including channel height, length, width, and device location. A constant heat flux was simulated for the devices, and the maximum allowable junction temperature for any device was set to 175°C. Two heat fluxes were investigated: one for an inverter with nine modules and a higher flux for an inverter with six modules (lower weight and volume, but higher current and losses in each device). From this study, an optimized design was selected that met the specific power and power density targets [15].

Sub-module heat exchangers, which represent one-sixth of a full module, were prototyped for the baseline and optimized geometries from 6063 aluminum using wire electrical discharge machining (see Figure 1). For significant volumes, final module-level heat exchangers could be manufactured using extrusion methods. Channels for both baseline and optimized configurations were 2 mm wide with 1-mm thick fin walls. The baseline channels were 15 mm tall and 74 mm long. The optimized channels were 21 mm tall and 40 mm long. The material thickness between the channels and the devices was 2.8 mm, calculated to nearly match the thermal resistance of a
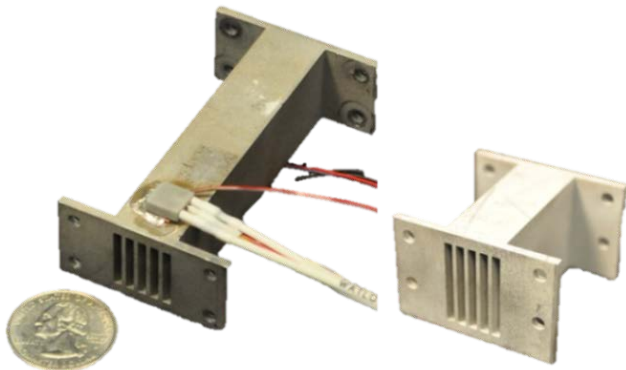
1

Fig. 1. Baseline (left) and optimized (right) sub-module heat exchangers fabricated from 6063 aluminum. Heaters are mounted on the top and bottom of the test section, one near the inlet edge and the other farther back. The flanges are for experimental convenience in attaching the test section to the inlet and outlet manifolds.

direct-bond-copper or direct-bond-aluminum substrate layer.

The test bench for this project used compressed air which was dried with a desiccant dryer to a dew point of -20°C or lower. The air was then passed through a 5-μm particulate filter and regulated at a pressure of 68 to 137 kPa. A mass flow controller provided flows of 3.3 to 166 cm^3/s. A downstream laminar flow element was used to more accurately measure the flow rate and feedback to control the mass flow controller. The air passed through a plate heat exchanger for temperature control and entered the heat exchanger test section, shown in Figure 2. Ceramic resistance heaters (8 mm × 8 mm) provided the heat load; power was adjusted to yield the desired junction temperature for each flow rate. A 0.5-mm copper base plate with an embedded thermocouple was attached with thermal epoxy to the test section. Indium foil was placed
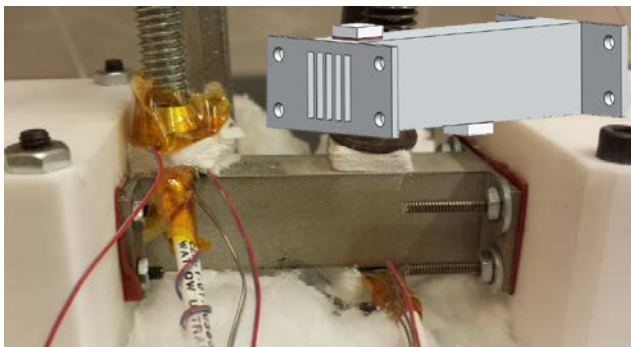

Fig. 2. Baseline aluminum sub-module test section. Ceramic resistance heaters providing the heat load are located on the top left and bottom right of the test section. Air flows from left to right.

between the copper base plate and the heater, topped with insulation, and held in place with a clamp. Exhaust air passed through porous aluminum foam to mix the air and achieve an accurate outlet temperature. The test section was wrapped in insulation. For more details of the experimental setup, see Waye et al. [15].

Tests were conducted over a range of flow rates. The power supplied to the heaters (dissipated as heat) and the pressure drop were measured for each flow rate. The heat dissipation and pressure drop results were extrapolated from the sub-module level to inverter scale; one module consisted of six sub-modules and nine or six modules made up the entire inverter for the baseline and optimized configurations, respectively.

Weights and volumes of inverter components were combined with the heat exchanger assembly to estimate the total weight and volume. The casing for each module was scaled for the heat exchanger geometry. The bus bars were assumed to be 0.088 kg per module. The capacitor was assumed to be 1.62 kg and 1.13 L. The gate driver and control board were assumed to be 0.42 kg and 0.88 L. Figure 3 shows the module-level heat exchanger and inverter assembly.
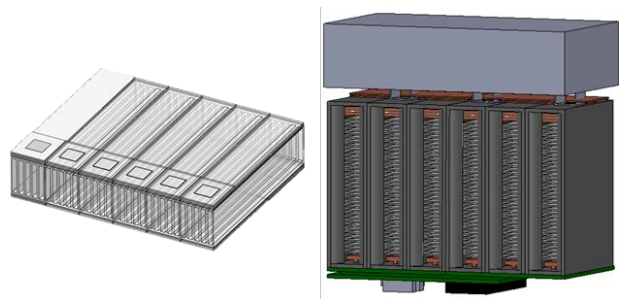

Fig. 3. Schematic of module-level heat exchanger (left) with devices (six on top, six on bottom), and six-module inverter (right) including module casing, capacitor, bus bars, control board, and gate driver board. Computational fluid dynamics and experiments were conducted on the sub-module heat exchanger (opaque portion on far left of module-level heat exchanger).

The parasitic power of the system was of interest. Pressure drops across two production ducts (from other air intake systems) were combined to act as a surrogate inlet and exhaust ducting path for the air-cooled inverter system [13]. The total pressure drop of the system was calculated by using the flow rate through the heat exchanger.

III. RESULTS AND DISCUSSION

The two production ducts for other applications were tested for pressure loss as a function of flow rate (Figure 4). The ducting path would be designed for each vehicle
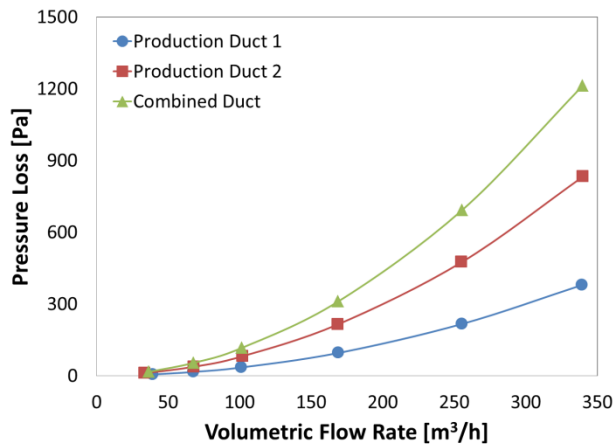
2

Fig. 4.   Pressure drop through two air intake ducts, acting as a surrogate ducting system. The pressure drop as a function of flow rate is added to the pressure drop of the heat exchanger for total pressure drop.

platform and vary, so these ducts provide an estimate of the air intake and exhaust pressure losses.

The heat dissipation for the baseline and optimized configurations is shown in Figure 5. Error bars represent 95% certainty levels. The target heat dissipation rate was 2.7 kW, which equates to an approximately 95% efficient inverter at peak power (55 kW). For the baseline configuration with nine modules, an approximate airflow of 100 m³/h [55 ft³/min] meets this target. The power density and specific power for this inverter would be 10.1 kW/L and 9.4 kW/kg, respectively. The fluid power (the product of flow rate and pressure drop, a parasitic load) is approximately 4 W. By reducing the number of modules to six and using a more efficient heat exchanger design,

the optimized configuration rejected 2.7 kW of heat at an approximate airflow rate of 350 m³/h [200 ft³/min]. The power density and specific power of the inverter rose to 14.5 kW/L and 14.6 kW/kg, but increased fluid power to approximately 110 W. Performance metrics are listed in Table 1. For each case, a fan must be sized to provide the fluid power, and the fan efficiency must be considered. A typical air conditioning system blower or compressor fan uses up to around 150 W at peak demand.

Table 1. Baseline and optimized inverter configuration performance metrics.

	Baseline (9 modules)	Optimized (6 modules)
Power Density [kW/L]	10.1	14.5
Specific Power [kW/kg]	9.4	14.6
Outlet Temperature [°C] at 2.7 kW heat dissipation	100	65
Flow Rate [m³/h] at 2.7 kW heat dissipation	100	350
Fluid Power [W]	4	110

The inlet temperatures for the experiments were between 40°C and 45°C. The variance was due to experimental control of a liquid bath used to heat the inlet air. Future tests may be conducted to at an inlet temperature of 50°C, which would represent extreme cases in ambient temperature. The outlet temperature decreases with increased flow rate, as seen in Figure 6. When the heat exchanger dissipated 2.7 kW of heat, the outlet temperature for the baseline configuration was approximately 100°C. The optimized configuration outlet temperature was approximately 65°C. Lower exhaust temperatures can be translated into less strenuous exhaust ducting requirements because vehicle under-hood temperatures can reach 150°C.
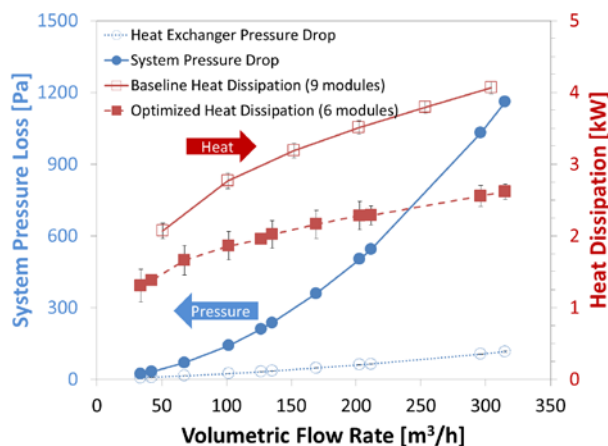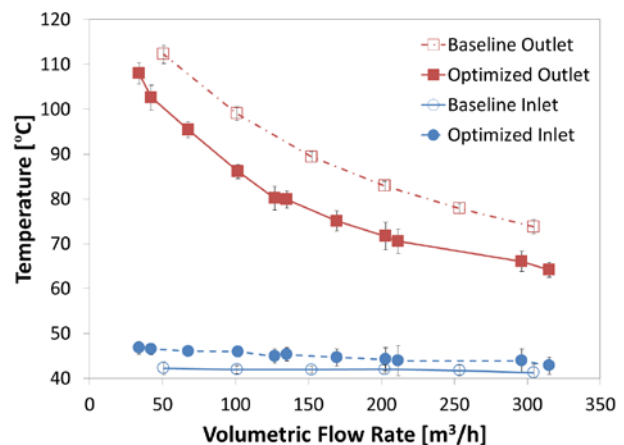

Fig. 5.   Heat dissipation curves and system pressure loss as a function of flow rate for the baseline nine-module inverter and optimized six-module inverter configurations. The target heat dissipation is 2.7 kW.

Fig. 6.   Inlet and outlet air temperatures as a function of flow rate for the baseline and optimized configurations.

3

IV. CONCLUSIONS

This study demonstrates an air-cooled inverter configuration using an optimized heat exchanger in an inverter with fewer modules that meets 2015 targets of 12 kW/L and 12 kW/kg. 2020 targets of 14.1 kW/L and 13.4 kW/kg were also met. Wide-bandgap materials enable smaller and higher performance devices that can operate at higher temperatures. The maximum junction temperature of 175°C, representing high-temperature devices such as silicon carbide or gallium nitride, enable air-cooling technology to be a viable candidate for automotive electric traction drive inverter applications.

Packaging employing lower junction temperatures, such as 150°C, could still use this air-cooled heat exchanger design, but less heat will be dissipated. Conversely, higher junction temperatures exceeding 200°C will increase heat dissipation or provide the same heat dissipation at lower flow rates and parasitic power. Higher inlet temperatures will lower the heat dissipation capacity slightly for the same flow rates.

Keeping the design simple, using light-weight materials, and leveraging manufacturing methods such as extrusion can keep costs low.

The geometry can be further optimized while ensuring compatibility with the electrical topology. Heat exchanger designs that efficiently dissipate heat while keeping flow rates low are more desirable than a high flow, low pressure-drop heat exchanger. The pressure drop of ducting dominates the system pressure drop, so a lower flow rate yields a lower system parasitic fluid power requirement.

REFERENCES

[1] "Semikron Application Manual 1998" http://www.semikron.com/skcompub/en/application_manual_2010-4165.htm. Section 3.1. Accessed on April 16, 2014.

[2] S. Matsumoto, "Advancement of hybrid vehicle technology," *European Conference on Power Electronics and Applications,* Dresden, Germany, September 2005.

[3] T. Uesugi and T. Kachi, "GaN power switching devices for automotive applications," *CSMan Tech Conference*, Tampa, Florida, May 2009.

[4] F. Renken and R. Knorr, "High temperature electronics for future hybrid powertrain application," *European Conference on Power Electronics and Applications*, Dresden, Germany, September 2005.

[5] T. Funaki, J. Balda, J. Junghans, A. Kashyap, H. Mantooth, F. Barlow, T. Kimoto, and T. Hikihara, "Power conversion with SiC devices at extremely high ambient temperatures," *IEEE Transactions on Power Electronics*, vol. 22(4), pp. 1321–1329, 2007.

[6] W. Nakayama, "Exploring the limits of air cooling," *Electronics Cooling*, vol. 12, no. 3, pp. 10-17, 2006.

[7] P. Rodgers, V. Eveloy, and M.G. Pecht, "Limits of air-cooling: status and challenges," *IEEE Semi-Therm Symposium*, San Jose, CA, March 2005.

[8] R.H. Staunton, T.A. Burress, and L.D. Marlino, *Evaluation of 2005 Honda Accord Hybrid Drive System*. ORNL/TM-2006/535. Oak Ridge, TN: Oak Ridge National Laboratory, September 2006.

[9] Y. Chow (media contact), "AC propulsion partners with BMW to build 500 electric vehicles." Press release. 2008. http://www.acpropulsion.com/pressreleases/11.20.2008%20BMW%20Press%20Release.pdf. Accessed July 6th, 2011.

[10] K. Kodani, T. Tsukinari, and T. Matsumoto, "New power module concept by forced-air cooling system for power converter." *IEEE 2010 International Power Electronics Conference*, Sapporo, Japan, July 2010.

[11] D. Bortis, B. Wrzecionko, and J.W. Kolar, "A 120°C ambient temperature forced air-cooled normally-off SiC JFET automotive inverter system." *IEEE 26th Annual Applied Power Electronics Conference and Exposition (APEC)*, Fort Worth, TX, March 2011.

[12] B. Wrzecionko, J. Biela, and J. Kolar, "SiC power semiconductors in HEVs: Influence of junction temperature on power density, chip utilization and efficiency." *IEEE 35th Annual Industrial Electronics Conference,* Porto, Portugal, November 2009.

[13] M. Chinthavali, "Gas cooled traction drive inverter," U.S. Patent No. 8,553,414 B2, issued October 8, 2013).

[14] "Electrical and Electronics Technical Team Roadmap," U.S. DRIVE, http://www1.eere.energy.gov/vehiclesand fuels/pdfs/program/eett_roadmap_june2013.pdf, June 2013

[15] S. Waye, S. Narumanchi, J. Lustbader, K. Bennion, and C. Smith, "Air-cooling technology for power electronics thermal management," FY2013 EERE Vehicle Technologies Office Advanced Power Electronics and Electric Motors Annual Report, April 2014.

4